SYNTHESIS AND CHARACTERIZATION OF NICKEL NANOPARTICLES VIA POLYOL METHOD FOR BIOMEDICAL APPLICATION

NIK ROSELINA BINTI NIK ROSELEY

UNIVERSITI SAINS MALAYSIA

July 2011

SYNTHESIS AND CHARACTERIZATION OF NICKEL NANOPARTICLES VIA POLYOL METHOD FOR BIOMEDICAL APPLICATION

by

NIK ROSELINA BINTI NIK ROSELEY

Thesis submitted in
fulfilment of the
requirements for the
Degree of Master of Science

July 2011

Declaration

I declare that this thesis is the result of my own research, that it does not incorporate without acknowledgement any material submitted for the degree or diploma in any university and does not contain any materials previously published, written or produced by another person except where due references are made in the text.

Signature:

Candidate’s Name:

Date:

Signature:

Supervisor’s Name:

Date:

ACKNOWLEDGEMENTS

In the name of Almighty Allah, The Compassionate, The Merciful.

I wish to thank first and foremost, Assoc. Prof. Dr. Azizan Aziz for his continues support, guidance throughout the project at every turn, encouraging me with his very valuable suggestions and for giving me this great opportunity to work with him. This research would not have been fruitful without the valuable suggestions and advices by Dr. Zainovia Lockman. I also owe my gratitude to all staff of School of Material and Mineral Resources Engineering, USM technicians especially Mrs. Fong Lee Lee, Mrs. Haslina, Mr. Zulkurnain, Mr. Zaini, Mr. Azrul, Mr. Rashid, who have been gracious in providing me with the laboratory facilities necessary to pursue the thoughts and ideas into practical existence, . As well as the staff of Electron Microscopy Laboratory, School of Biology, USM: especially M. Muthu and Mrs. Faizah for the supports and encouraging ideas. School of Material and Mineral Resources Engineering administrative office: Ms. Hakisyah, Mrs. Jamilah, and the rest in the office have been assisting me directly or indirectly throughout my life in the school.

My special thanks are dedicated to the people in my personal life: three most important people in my life, husband, Mohd Najib Samsuri, princess, Damia Qistina and prince, Danish Qasyri whose loves and supports made all this possible. I wish to thank my wonderful parents, Nik Roseley Nik Mohamed and Maznah Mohammad and my family members for their endless support over the years. I also wish to express my acknowledgement to my laboratory colleague, Khe Cheng Seong, Siti

Norzidah, Khairunisa, Suriati and other friends for the precious discussions and talks, inspiration and cheering up my life these past years.

I would also like to express my deepest gratitude to Universiti Sains Malaysia, School of Material and Mineral Resources Engineering, USM-RU-PGRS grant number 1001/PBahan/8031022, Universiti Teknologi MARA for the opportunity, equipments and financial support in pursuing my Master Degree. My grateful also dedicated to AMREC- SIRIM for their valuable advice and expertise on VSM and XPS analyses.

TABLE OF CONTENTS

	PAGE
ACKNOWLEDGEMENTS	ii
TABLE OF CONTENTS	iv
LIST OF TABLES	ix
LIST OF FIGURES	xii
LIST OF ABBREVIATIONS	xxi
LIST OF SYMBOLS	xxii
ABSTRAK	xxiii
ABSTRACT	xxiv
CHAPTER 1: INTRODUCTION	
1.1 Background of the study	1
1.2 Objective	4
1.3 Scope of work	5
CHAPTER 2: LITERATURE REVIEW	
2.1 Introduction to nanotechnology	6
2.2 Nanoscale materials	7
2.3 Ni Bulk vs. Nano	
2.3.1 Overview	7
2.3.2 Crystallite structure	8
2.3.3 Ni nanostructures particles	11
2.4 Synthesis of metal nanoparticles	
2.4.1 Overview	13

2.4.2 Preparation of Ni nanoparticles 14

2.4.3 Microemulsion method 14

2.4.4 Polyol Method 15

2.5 Influence of experimental parameters on the synthesis of nanoparticles

2. 5.1 Overview 18

2. 5.2 Effect of Temperature 19

2. 5.3 Effect of pH 21

2. 5.4 Effect of Reducing agent 22

2. 5.5 Effect of reaction time 23

2. 5.6 Effect of metal precursor concentration 24

2. 5.7 Reduction, nucleation and growth 25

2. 5.8 Method of mixing of reactants 27

2. 5.9 Protective agents/capping agents 28

2.6 Bimetallic nanoparticles

2.6.1 Introduction 29

2.6.2 Synthesis of Bimetallic 31

2.6.3 Characterization of bimetallic nanoparticles 35

2.7 Optical Properties

2.7.1 Overview 38

2.7.2 Surface plasmon resonance of Ni and other metal nanoparticles 39

2.7.3 Surface plasmon resonance of bimetallic structure 41

2.8 Magnetic Properties

2.8.1 Classification of magnetism 43

2.8.2 Magnetization curve and hysteresis 45

2.8.3 Magnetic property of Ni nanosize materials 47

2.8.3 Magnetic properties of Ni nanostructured 50

2.7.4 Magnetic properties of Ni bimetallic structures 51

2.9 Application of magnetic nanoparticles

2.9.1 Introduction 52

2.9.2 Applications of Ni nanoparticles 53

2.9.3 Potential application of Ni@Au bimetallic structure 54

CHAPTER 3: MATERIALS AND METHODS

3.1 Introduction 56

3.2 Raw Materials 57

3.3 Preparation of Reactant Solutions 58

3.4 Synthesis of Ni nanoparticles at 60˚C 59

3.4.1 Effect of N_2H_4/Ni^{2+} molar ratio 60

3.4.2 Effect of OH^-/Ni^{2+} molar ratio 60

3.4.1 Effect of addition sequence of reactants 61

3.5 Synthesis of Ni nanoparticles at boiling point of EG 62

3.5.1 Effect of addition sequence of reactants 62

3.5.3 Effect of OH^-/Ni^{2+} molar ratio 63

3.5.5 Effect of reaction time 63

3.6 Synthesis of Ni@Au bimetallic 64

3.7 Washing of precipitate 66

3.8 Characterizations 67

3.8.1 Transmission Electron Microscopy (TEM) 67

3.8.2 Field –Emission Scanning Electron Microscopy (FE-SEM) 68

3.8.3 X-ray Diffraction (XRD) 69

3.8.4 Fourier Transform Infrared (FTIR) 70

3.8.5 UV-Vis 70

3.8.6 Room-temperature Magnetic Measurements 71

3.8.7 X-ray photospectroscopy (XPS) 71

3.8.8 Zeta Potential 72

CHAPTER 4: RESULTS AND DISCUSSION

4.1 Introduction 73

4.2 Synthesis of Ni nanoparticles at 60˚C 73

4.2.1 Effect of N_2H_4/Ni^{2+} molar ratio 73

4.2.2 Effect of OH^-/Ni^{2+} molar ratio 83

4.2.3 Effect of mode of addition of reactants 94

4.3 Synthesis of Ni nanoparticles at boiling point of EG 102

4.3.1 Effect of addition sequence of reatants 103

4.3.2 Effect of OH^-/Ni^{2+} molar ratio 106

4.3.3 Effect of synthesis time 121

4.4 Synthesis of Ni@Au bimetallic structure 131

4.6 Room-temperature magnetic properties of as-synthesized products 144

4.6.1 Influence of particles size on magnetic properties 145

4.6.2 Magnetic properties of bimetallic structures 148

4.6.3 Influence of precipitates morphologies on magnetic properties 151

CHAPTER 5: CONCLUSIONS AND RECOMMENDATIONS

5.1 Introduction 153

5.2 Conclusions 153

5.3 Recommendations for future research 155

REFERENCES 156

APPENDICES:

APPENDIX A

APPENDIX B

LIST OF PRESENTATIONS AND PUBLICATION

APPENDICES

APPENDIX A

EXPERIMENTAL SETUP

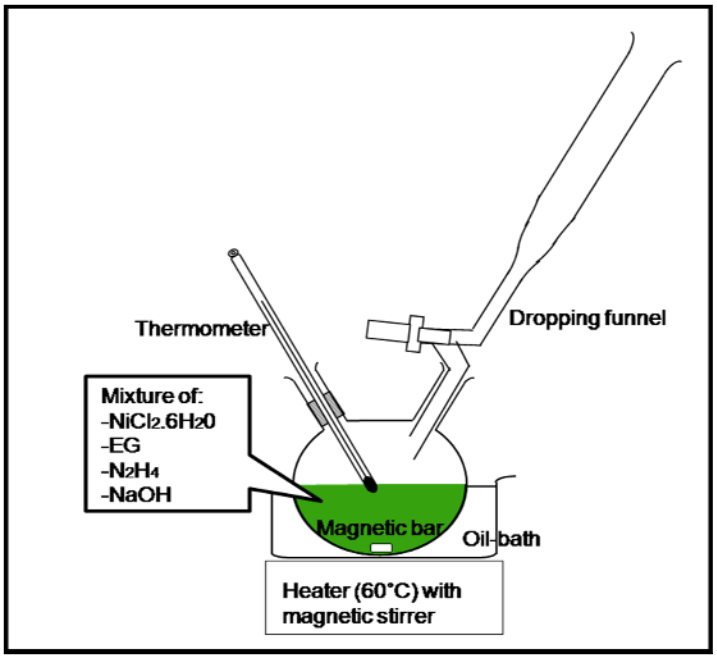

Figure A1 Experimental setup of synthesis of Ni nanoparticles in 60˚C.

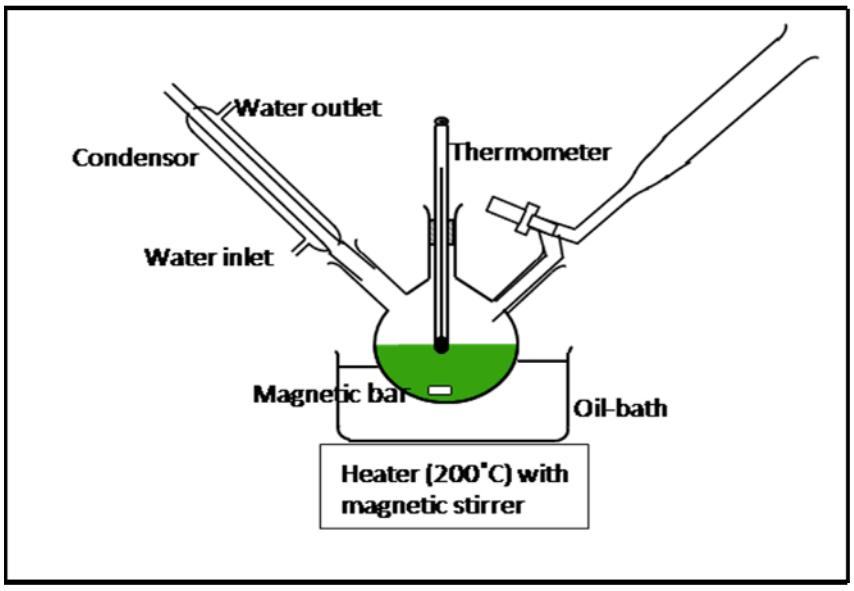

Figure A2 Experimental setup of synthesis of Ni nanoparticles in boiling temperature of EG

APPENDIX B

MICROGRAPHS OF BIMETALLIC PARTICLES (CS1)

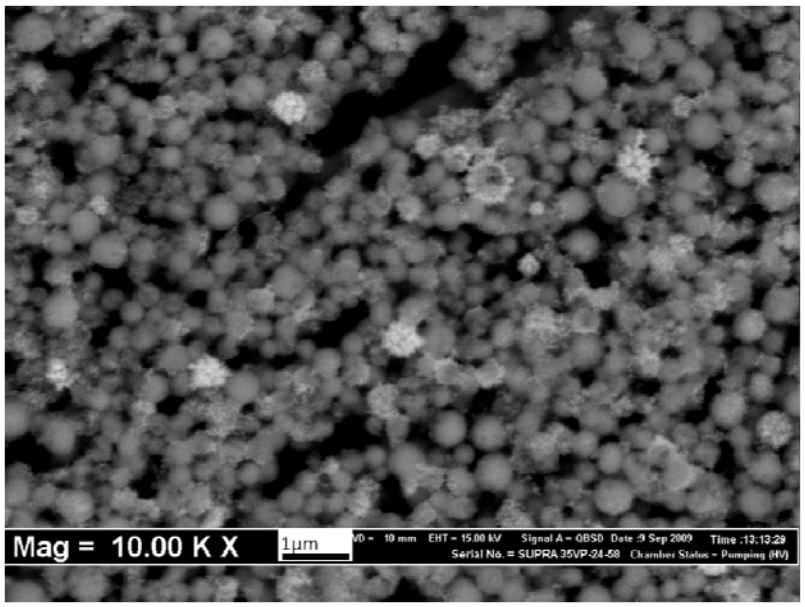

Figure B1 FE-SEM (backscattered) micrograph of sample CS1.

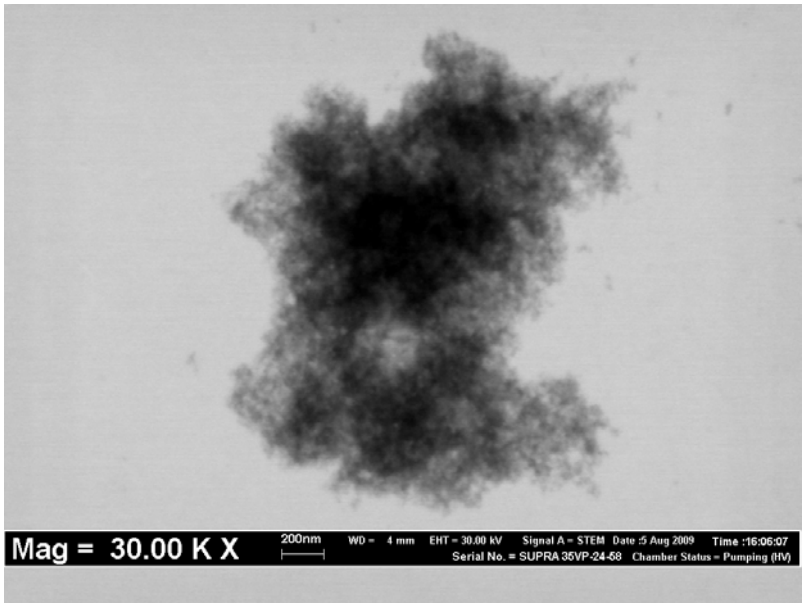

Figure B2 STEM micrograph of sample CS1.

LIST OF TABLES

		PAGE
Table 2.1	Standard reduction potential of selected metals	34
Table 2.2	Overview of coercivity, Hc and saturation Magnetization, Ms at room temperature for various sizes of Ni nanoparticles	49
Table 2.3	Saturation Magnetization (Ms) at 300K for various morphologies of Ni nanostructures	50
Table 2.4	Saturation Magnetization (Ms) at room temperature for several type of Ni bimetallic structured	52
Table 3.1	Raw materials used to synthesis Ni and Ni@Au nanoparticles	58
Table 3.2	Reactant concentrations and N_2H_4/Ni^{2+} molar ratios investigated	60
Table 3.3	Reactants concentration and OH^-/Ni^{2+} molar ratios investigated	61
Table 3.4	Experimental condition employed to study the effect of mode of addition	61
Table 3.5	Experimental condition employed to study the effect of mode of addition	63
Table 3.6	Reactants concentration and OH^-/Ni^{2+} molar ratios investigated	63
Table 3.7	Reactants concentration and reaction time investigated	64

Table 3.8	PH of mixture investigated	66
Table 3.9	Ni/Au molar ratios investigated	66
Table 4.1	Recorded observations of colour changes during synthesis and the calculated crystallite size of each samples	80
Table 4.2	Recorded observation for each set of combination of concentration	81
Table 4.3	Elements weight percentage from EDX analysis for each sample	89
Table 4.4	Observation of final colour, pH and calculated crystallite size of each sample	93
Table 4.5	Recorded reaction time and final colour of each sample	96
Table 4.6	Obtained FTIR absorbance spectrums of pure EG, 30 mM $NiCl_2$, 1 M NaOH and 0.15 M N_2H_4 diluted in EG at room temperature (RT)	100
Table 4.7	Proposed reduction pathway for different mode of addition	102
Table 4.8	Recorded reaction time and the final colour	103
Table 4.9	Recorded observation of colour and reaction time for each sample	114
Table 4.10	Calculated mean particles size and standard deviation obtained from TEM analysis of Ni particles at different reaction time.	128

Table 4.11	Recorded observation and colour of supernatant for bimetallic samples	132
Table 4.12	Recorded observation of the colour of post reaction and supernatant colours for different Ni/Au molar ratios	137
Table 4.13	Coercivity (Hc), saturation magnetization (Ms) and remanent magnetization (Mr) of different sizes of Ni particles	148
Table 4.14	Coercivity (Hc), saturation magnetization (Ms) and remanent magnetization (Mr) of bimetallic structures	150
Table 4.15	Coercivity (Hc), saturation magnetization (Ms) and remanent magnetization (Mr) of nano-structures particles	152

LIST OF FIGURES

		PAGE
Figure 2.1	Selected-area electron diffraction (SAED) pattern for fcc Ni nanocrystallites with size of 2 nm (Zach and Penner, 2000)	8
Figure 2.2	XRD patterns of (a) Ni and $Ni(OH)_2$ mixture and (b) pure Ni (Abdel-Aal et al., 2007)	9
Figure 2.3	Ni nanostructured have been synthesized with the following shapes: (a) Sea urchin-like Ni, (b) Needle-like Ni, (c) Dandelion-like Ni, (d) Ni flowerlike, (e) Ni nanorod (Modified from Hu and Sugawara, 2008; Zhang et al., 2005; Tian et al., 2005; Wang et al., 2008; Yu et al., 2006)	12
Figure 2.4	Ni self-assembly of (a) nanoflowers, (b) snow-ball flower, (c) nanowires (Modified from Xu et al., 2008; Mandal et al., 2009; Wang et al., 2009)	12
Figure 2.5	Model representation of (a) Bottom-up approach and (b) Top-down approach	13
Figure 2.6	The HOMO and LUMO energy levels for TMEG and EG on comparison with SOMO for metal salts (Joseyphus et al., 2007)	16
Figure 2.7	Schematic presentation of the different stages of the reaction process in polyol synthesis (Kim et al., 2009)	17
Figure 2.8	Schematic representation of nanoparticles synthesis (Shevchenko et al., 2003)	20
Figure 2.9	Schematic of Oswalt ripening process	24

Figure 2.10	LaMer diagram as a schematic explanation for the formation process of monodispersed particles. C_{∞} and C_{crit} are the equilibrium concentration of solute with the bulk solid and the critical concentration as the minimum concentration for nucleation, respectively. Region I,II and III represent the prenucleation, nucleation and growth stages respectively (Sugimoto, 2007)	26
Figure 2.11	Synthesis of monodisperse nanoparticles by the injection of reagents into hot surfactant solution (Hyeon, 2003)	28
Figure 2.12	Cross-sections of models for PVP-stabilized Au-Pd (1: 1) bimetallic nanoparticles : (a) Au single-core-Pd shell model, (b) cluster-in-cluster model, (c) random model (Toshima et al., 1992)	30
Figure 2.13	TEM images of nanoshell growth on 120 nm diameter silica dielectric nanoparticle. a. Initial gold colloid-decorated silica nanoparticle, b.–_e. Gradual growth and coalescence of gold colloid on silica nanoparticle surface, f. Completed growth of metallic nanoshell (Oldenburg et al., 1998)	33
Figure 2.14	Schematic of Core-Shell Nanoparticle Formation via Redox Transmetalation Processes (Lee et al., 2005)	34
Figure 2.15	Redox reaction of Co-Au nanoparticles (Mandal and Krishnan, 2006)	35
Figure 2.16	Ni@Pt core@shell nanoparticles (Ahrenstorf et al., 2008)	36
Figure 2.17	SAED pattern of Co@Au nanoparticles (Cheng and Walker, 2007)	37

Figure 2.18	HRTEM image of core-shell Au@Pd (Harpeness and Gedanken, 2004)	37
Figure 2.19	EELS spectra of 9 nm diameter Co-Au core-shell nanoparticles from (a) center and (b) edge	37
Figure 2.20	Size dependence of the colloids colour for Au (Parash, 2010)	39
Figure 2.21	UV-vis spectra recorded from: curve 1, cobalt nanoparticle solution; curve 2, as-synthesized Co@Au nanoparticle solution; curve 3, aqueous solution of pure $CoCl_2$. The inset shows the UV-vis spectrum after subtracting curve 3 from curve 2 in the main figure (Mandal and Krishnan, 2006)	40
Figure 2.22	UV-Vis absorption spectra for Ni@Ag bimetallic at different molar ratio (Lee et al., 2009)	41
Figure 2.23	Calculated optical resonances of silica core, Au shell nanoshells over a range of core radius@shell thickness ratios. Sizes in figure indicate Au shell thickness with 60 nm core radius (Halas, 2002)	42
Figure 2.24	A periodic table showing the type of magnetic behaviour of each element at room temperature	44
Figure 2.25	Particles size vs. coercivity (Talapin et al., 2004)	45
Figure 2.26	Schematic of M-H loop in a ferromagnetic material showing the coercive field, Hc, saturation magnetisation, Ms and remanent magnetisation, Mr	46
Figure 2.27	Plots of coercivity of Ni nanoparticles vs. average particle size at room temperature (Wang et al., 2008)	49

Figure 2.28	M-H loop of nanopowders of different morphologies (Wang et al., 2008)	50
Figure 2.29	The M-H loop of Ni-Ag alloy (Lee et al., 2009)	51
Figure 2.30	Multifunctional magnetic nanoparticles and their potential applications (Gao et al., 2009)	53
Figure 2.31	Base-metal-electrode multilayer ceramic capacitor (BMLL) (Source: From www.paumanokgroup.com)	54
Figure 2.32	Illustration of thermotherapy strategy using magnetic nanoparticles (Ito et al., 2005)	55
Figure 3.1	Flow chart showing the experimental procedure of the synthesis of Ni nanoparticles in 60˚C temperature	59
Figure 3.2	Flow chart showing the experimental procedure of the synthesis of Ni nanoparticles in 60˚C temperature	62
Figure 3.3	Flow chart showing the experimental procedure of the synthesis of Ni@Au bimetallic nanoparticles	65
Figure 4.1	Typical TEM micrographs of sample (a) R5, (b) R10, (c) R20 and (d) R30	75
Figure 4.2	Typical FE-SEM micrograph of sample R30. [Ni2+] = 0.1M; [N2H4] = 12M; N_2H_4/Ni^{2+} molar ratio = 30	76
Figure 4.3	XRD patterns of sample (a) R5 (N_2H_4/Ni^{2+} = 5), (b) R10 (N_2H_4/Ni^{2+} = 10), (c) R20 (N_2H_4/Ni^{2+} = 20), (d) R30 (N_2H_4/Ni^{2+} = 30). The inset shows the two small peaks of Ni-complex for sample R30 mark as Δ	77

Figure 4.4	Schematic illustrate the production of Ni metal from (a) Ni complex to $Ni(OH)_2$ and (b) when using excess hydrazine to produce mixture of Ni metal and Ni-complex	79
Figure 4.5	Typical TEM micrographs of samples (a) sample #1 ($[Ni^{2+}]$= 5mM, $[N_2H_4]$= 50 mM), (b) sample #2 ($[Ni^{2+}]$= 10 mM, $[N_2H_4]$= 1 M)	82
Figure 4.6	SEM micrographs of sample (a) P4, (b) P8, (c) P10 and (d) P20	84
Figure 4.7	High magnification SEM micrograph of ball wool-like particles showing the estimated diameter and length of each nanochain that formed the submicron particles	85
Figure 4.8	Low magnification of typical FE-SEM micrographs for sample (a) P8, (b) P10 and (c) P20	87
Figure 4.9	(a) STEM micrograph of sample P10, (b) TEM micrograph of sample P20	88
Figure 4.10	EDX analyses for sample (a) P8, (b) P10 and (c) P20	89
Figure 4.11	XRD patterns of (a) P0 (OH^-/Ni^{2+} = 0), (b) P4 (OH^-/Ni^{2+} = 4), (c) P8 (OH^-/Ni^{2+} = 8), (d) P10 (OH^-/Ni^{2+} = 10), (e) P20 (OH^-/Ni^{2+} = 20)	91
Figure 4.12	A proposed pathway to the growth mechanism of ball wool-like nanostructure	94
Figure 4.13	TEM and STEM micrographs of sample (a) M2-L and (b) M3-L respectively	97

Figure 4.14	FT-IR spectrums of (a) pure EG, (b) 30 mM $NiCl_2$, (c) 1M NaOH and (d) 0.15M N_2H_4 diluted in EG at room temperature (RT)	99
Figure 4.15	FT-IR spectrums of (a) $NiCl_2$-NaOH-EG, (b) $NiCl_2$-EG	101
Figure 4.16	FT-IR spectra of (a) N_2H_4-EG and (b) N_2H_4-EG after heat to boil with reflux.	105
Figure 4.17	TEM micrographs of sample (a) M1-H, (b) M2-H and (c) M3-H	105
Figure 4.18	TEM micrographs of sample (a) Prf0 (OH^-/Ni^{2+} = 0), (b) Prf4 (OH^-/Ni^{2+} = 4), (c) Prf8 (OH^-/Ni^{2+} = 8), (d) Prf10 (OH^-/Ni^{2+} = 10) and (e) Prf 20 (OH^-/Ni^{2+} = 20)	108
Figure 4.19	Particles size distributions for samples (a) Prf0 (d_{mean}= 4.11 nm), (b) Prf4 (d_{mean}= 5.43 nm), (c) Prf8 (d_{mean}= 4.37 nm), (d) Prf10 (d_{mean}= 4.13 nm) and (e) Prf20 (d_{mean}= 4.03 nm)	110
Figure 4.20	Plot of mean particles size against mole ratio of Ni^{2+} to OH^-	111
Figure 4.21	XRD patterns of samples (a) Prf0, (b) Prf4, (c) Prf8, (d) Prf10 and (e) Prf20. • = FCC Ni	112
Figure 4.22	FT-IR spectrums of supernatant for samples (a) Prf0, (b) Prf4, (c) Prf8, (d) Prf10 and (e) Prf20	115
Figure 4.23	Typical STEM micrographs of samples (a) Prf0, (b) Prf4, (c) Prf10, (d) Prf20	118
Figure 4.24	Typical FE-SEM micrograph of sample Prf10	119

Figure 4.25	Zeta Potential of samples (a) Prf0, (b) Prf4, (c) Prf8, (d) Prf10 and (e) Prf20	120
Figure 4.26	Photographs of colour changes of solution taken randomly start from immediate after injection of ($NiCl_2$ + NaOH) mixture until heating was stopped after 2 hours synthesis	122
Figure 4.27	Photographs of as-synthesized products taken at (a) 5 min, (b) 15 min, (c) 1 hr and (d) 2 hr reaction time	123
Figure 4.28	TEM micrographs of (a) D5 (t = 5 min), (b) D15 (t = 15 min), (c) D60 (t = 1hr) and (d) D120 (t = 2hrs) respectively	124
Figure 4.29	Particles size distributions histogram of (a) D15, (b) D60 and (c) D120. Size distribution was determined by counting 100 particles using ImageJ software	126
Figure 4.30	XRD patterns of (a) D5 (t = 5 min), (b) D15 (t = 15 min), (c) D60 (t = 1 hr) and (d) D120 (t = 2 hrs). Inset is the details of diffraction pattern of sample D5 (★ = NiO, ◊ = $Ni(OH)_2$)	127
Figure 4.31	UV-Vis spectrums of samples (a) D5 (t = 5 min), (b) D15 (t = 15 min), (c) D60 (t = 1 hr) and (d) D120 (t = 2 hrs) Schematic diagram of the reaction procedure at different reaction times.	129
Figure 4.32	Schematic diagram of the reaction procedure at different reaction times for this particular concentration in this work	130
Figure 4.33	Typical TEM micrographs of (a) Ni nanoparticles as core and (b) as-synthesized Au with the same concentration used for sample CS1	133

Figure 4.34	TEM micrographs of samples (a) CS1 and (b) CS2	134
Figure 4.35	FE-SEM micrographs of dried powder of sample (a) CS1 and (b)CS2	135
Figure 4.36	Elemental analyses of sample (a) CS1; Wt% CK=2.5, OK=2.5, NiL=41, AuM=54, Ni/Au= 0.8 and (b) CS2; Wt% CK=2.3, OK=2.1, NiL=72.5, AuM=23.1, Ni/Au=3.2	136
Figure 4.37	UV-visible spectrums of sample (a) CS1, (b) CS2, (c) physical mixture of Au and Ni, (d) pure Au particles and (e) pure Ni particles	138
Figure 4.38	UV-visible spectrums of (a) $NiCl_2$-EG before reaction, (b) supernatant of CS3 post reaction and (c) supernatant of CS1 post reaction	141
Figure 4.39	Wide XPS spectra of sample CS1 layer	143
Figure 4.40	Fitted XPS spectrum of (a) Ni 2p and (b) Au 4d regions for CS1 bimetallic nanoparticles	143
Figure 4.41	Schematic representation of two of the possible formations of Ni@Au bimetallic	144
Figure 4.42	Magnetization (emu/g) vs. applied magnetic field (Oe) for samples (a) D5 (sample mixture of very fine Ni nanoparticles and $Ni(OH)_2$), (b) D15 (1.84 nm), (c) D60 (6.5 nm) and (d) D120 (175.4 nm)	146
Figure 4.43	Plot of coercivity (Oe) of the Ni particles with different sizes	147

Figure 4.44	The effect of a permanent magnet on Ni@Au bimetallic nanoparticles. Observation over time was recorded as permanent magnet was placed by side of sample vial	148
Figure 4.45	Magnetization (emu/g) vs. applied magnetic field (Oe) for bimetallic structure samples (a) CS1 and (b) CS2	149
Figure 4.46	Magnetization (emu/g) vs. applied magnetic field (Oe) for the (a) Chain-like Ni structure and (b) Ball wool-like Ni structure	152

LIST OF ABBREVIATIONS

EDX	: Energy Dispersive X-ray Spectroscopy
EG	: Ethylene Glycol
FCC	: Face-Centered Cubic
FE-SEM	: Field Emission Scanning Electron Microscopy
FTIR	: Fourier Transform Infrared Spectroscopy
FWHM	: Full Width at Half Maximum
HCP	: Hexagonal Close-packed
KBM	: Kubik Berpusat Muka
TEM	: Transmission Electron Microscopy
UV-vis	: Ultraviolet- visible Spectroscopy
VSM	: Vibrating Sample Magnetometer
XRD	: X-ray Diffraction
XPS	: X-ray photoelectron spectroscopy

LIST OF PRESENTATIONS AND PUBLICATION

1. Nik Roselina, N.R., Azizan, A. and Lockman, Z. Facile and apid Synthesis of Nickel Colloidal Nanopaicles via Non-aqueous Polyol Method. Orally Presented for the International Conference of Nanotechnology. City Bayview Hotel, Langkawi, Kedah, Malaysia, December 2009.

2. Nik Roselina, N.R., Azizan, A. and Lockman, Z. Preparation of Ni nanoparticles: Controlling the degree of agglomeration by manipulating the molar ratio of hydrazine to metal precursor. Poster Presentation for the XAPP, Palace of Golden Horses, Seri Kembangan, December 2009.

3. Nik Roselina, N.R., Azizan, A. and Lockman, Z. Synthesis and Characterization of Ni nanoparticles. Poster Presentation for EMSM, Holiday Inn, Glenmarie, Selangor, December 2008.

4. Nik Roselina, N.R., Azizan, A. and Lockman, Z. Synthesis of Nickel Nanoparticles via Non-aqueous Polyol Method: Effect of reaction time. Sains Malaysiana. Under Review.

SINTESIS DAN PENCIRIAN NANOPARTIKEL NIKEL MELALUI KAEDAH POLIOL BAGI APLIKASI DALAM BIDANG BIOPERUBATAN

Abstrak

Potensi aplikasi Nanopartikel Nikel (Ni) terutamanya dalam bidang bioperubatan telah menarik minat banyak penyelidikan bagi memahami sepenuhnya proses penyediaannya. Tujuan utama projek ini adalah untuk menghasilkan Nanopartikel Ni yang berbentuk sfera dan berpermukaan licin serta taburan saiz yang kecil yang boleh ubah, melalui kaedah yang ringkas dan ekonomi. Proses ini diikuti dengan penyalutan Au bagi aplikasi dalam bidang bioperubatan. Kebanyakan kaedah yang telah dilaporkan biasanya melibatkan proses yang leceh, rendah kadar penghasilannya, mahal dan rumit. Bagi mengatasi masalah ini, projek ini menyampaikan pendekatan baru bagi menghasilkan nanopartikel Ni melalui kaedah poliol, menggunakan hidrazin sebagai agen penurun dan etilena glikol (EG) sebagai pelarut. Untuk proses penyalutan dengan Au, natrium sitrat bertindak sebagai agen penurun dan asid sitrat sebagai pengawal pH. Pencirian dilakukan dengan TEM, FE-SEM, EDX, XRD, UV-Vis, FTIR, XPS Zeta Potential dan VSM bagi mengkaji morfologi, saiz, struktur, komposisi kimia, serta sifat optikal, cas permukaan dan sifat magnet. Keputusan analisis menunjukkan KBM nanopartikel Ni yang berbentuk sfera dengan partikel paling kecil bersaiz 1.8 nm telah berjaya dihasilkan, serta saiznya boleh diubah dengan menambah tempoh tindak balas. Dari penelitian UV-Vis spektra, didapati partikel dwilogam Ni@Au bersaiz 26 – 40 nm telah berjaya disintesis melalui proses redoks-antaralogam dengan hadirnya puncak lebar pada lebih kurang 540 nm. Sukatan magnet pada suhu bilik menunjukkkan semua nanopartikel Ni dan dwilogam Ni@Au adalah bersifat feromagnet dengan nilai kepaksaan, Hc dan tepuan magnet bertambah dari 3.5 emu/g ke 19.1 emu/g bagi partikel bersaiz seperti di atas.

SYNTHESIS AND CHARACTERIZATION OF NICKEL NANOPARTICLES VIA POLYOL METHOD FOR BIOMEDICAL APPLICATION

Abstract

The diverse potential applications of nickel (Ni) nanoparticles especially in biomedical has driven intense research interest towards fully understanding the synthesis process. The aim of this work is to produce Ni nanoparticles with spherical shape and smooth surface, narrow in size distribution that can easily be tailored, through simple and economic procedure. The process followed by Au coating for biomedical application. Most of currently reported synthesis method of Ni nanoparticles usually involved tedius, low yield, expensive and complicated process. To overcome many of the limitations, we present new approach to synthesis Ni nanoparticles utilizing polyol method in the present of hydrazine as the reducing agent and ethylene glycol (EG) as the solvent. In the process of Au coating, sodium citrate acted as the reducing agent while acid citrate as the pH controller. As-synthesized products were characterized with TEM, FE-SEM, EDX, XRD, UV-Vis, FTIR, XPS, Zeta Potential and VSM to investigate the morphology, size, structure, chemical composition, surface charge, optical property as well as the magnetic property. The results indicated that spherical FCC Ni nanoparticles with the finest size of 1.8 nm had been successfully synthesized, and the size is tuneable by extending the reaction time. UV-VIS absorption spectra analysis suggested that Ni@Au bimetallic particles were produced via redox-transmetalation process with a very broad peak at about 540 nm and size range of 26 - 40 nm. Room temperature magnetic characterization of Ni nanoparticles shows typical ferromagnetic behaviour as well as the bimetallic structure with magnetization increased from 3.5 emu/g to 19.1 emu/g for particles size mentioned above.

CHAPTER 1

INTRODUCTION

1.1 Background of the study

Exploration in the studies of nanomaterials have attracted continues interest to many researchers throughout the world in expanding the knowledge of nanomaterials synthesis. Nanoparticle is favourite example of nanomaterials that can be found in many commercial applications nowadays. Ni is one of the important magnetic materials. The progressive research in the production of Ni in nanoscale range is due to the improvement that has been showed especially in the properties of magnetic, electrical conductivity and catalytic which promises future potential applications in the areas such high-density magnetic recording media. Recent studies also showed that magnetic nanoparticles such Ni possess unique magnetic properties to be applied in biomedical areas such as magnetic resonance imaging (MRI), drug delivery, therapeutic etc. It have been reported that particles with ferromagnetic or superparamagnetic can be manipulated by an external magnetic field which can drive them to the target areas such as cancer (Sun et al., 2008). By virtue of the nanometer-sized also, Ni nanoparticles have advantage of intelligently functioning in human biological body. Their properties when in nanoscale are well known to be extremely dependent on their size, morphology and method of preparation as well.

Precious elemental metal such as Co and Ni are very difficult to synthesize compare to noble metal like Au. Besides, their tendencies to agglomerate and oxidize are very high when they are in nanoscale. Although numerous methods have been reported, the mechanism and behavior of process that occur during synthesis are among the subject that yet to be fully understood. Most of reported methods usually

involved low yield, expensive and complicated procedure. These limitations have encouraged more studies to be carried out, in order to develop better method that could be applied for mass production purpose.

Despite Ni advantages and potential in biomedical application, it is actually highly toxic material and unlikely to be used as biomedical agent. This had created an idea and immense efforts to fabricate of bimetallic structure where the toxic nanoparticles will be coated with non-toxic and protective elements. Coating can prevent the leaking of potentially toxic component into human body (McBain et al., 2008). Investigations have largely been spurred as this new class of material could lead us nearer to its application in medical world. Among bimetallic nanoparticles, those containing Au or Ag are the most common and their preparations have been reported in several papers. By coating Ni nanoparticle with a stable noble metal like Au, Ni nanoparticles are also protected from oxidation. Au has become a favoured coating material because of a simple synthetic procedure and its chemical functionality. Further, since Au is diamagnetic the magnetic properties of nickel would not be adversely affected. In the synthesis of core@shell structures, strong reducing agent may promote rapid reduction of Au that prevents formation of a uniform shell. Instead of forming a shell on the core, individual Au nanoparticles, random alloy or cluster in cluster structures may also be produced. To form a uniform gold shell, it is critical to synthesize particles in a non-polar solvent under a mild reducing condition. Until this day, the numbers of reports on the fabrication of bimetallic nanoparticles are very few, thus it is very interesting and challenging to produce the bimetallic structure.

In order to produce Ni@Au bimetallic structure, the most significant challenge is Ni nanoparticles need to be spherical in shape, smooth surface, monodispersed and small in size. Ni nanoparticles of various morphologies and size have been reported to be produced via microemulsion, hydrothermal, polyol etc. The most interest is the spherical and well-distributed Ni nanoparticles. Compared to polyol method most of the other methods are either complicated or expensive. Polyol method developed by Fievet et al (1988) have the advantages of producing monodispersed, energy-efficient, environmental friendly, facile, cheap and are not susceptible to impurities. In polyol method, typically polyol such as ethylene glycol (EG) is used as the solvent and there is no need to use other protective agent. Protective agent such as PVP may change the surface properties of Ni and also create additional cost to the process. EG is also easy to be washed without any additional cleaning process like annealing (Wu and Chen, 2003). Synthesis of fine and monodispersed Ni nanoparticles have been developed through several modification of polyol method such as tailoring the temperature, pH, introducing stronger reducing and protective agent, time and many others.

In this work, we extend the polyol method to synthesis Ni nanoparticles without any protective agent. The synthesis will be divided into two main techniques which is synthesis at temperature of 60˚C and at boiling temperature of the polyol which is approximately 197˚C. Synthesis at 60˚C is a modified version of low temperature approached that has been reported by Chen and Wu (2003). Chen and Wu developed an interesting method of producing small yet monodispersed nanoparticles without the present of any other protective agent using mild reducing agent in relatively short reaction time of 1 hour. However they never presented how

experimental setup was carried out in capped bottle when N_2 gas was released in the process and also did not clearly stated how NaOH and hydrazine was diluted to certain concentration. In addition the reduction using relatively high concentration of hydrazine (0.05 – 0.9 M) might be considered as non economic as well as hazardous to human. On the other hand, synthesis at high boiling temperature of polyol use in this work is modification of the conventional method of polyol that do not used any reducing agent and need hours to complete reduction to modified polyol using mild concentration of reducing agent to promote the reduction process.

In order to verify the shape and size, as well as to analyze its properties, a few selected characterization techniques have been performed in this work. That include transmission electron microscopy (TEM), Field –Emission Scanning Electron Microscopy (FE-SEM), X-ray diffraction (XRD), Fourier Transform Infrared **(**FTIR), ultraviolet-visible (UV-Vis) spectrometer, Vibrating Sample Magnetometer (VSM), Zeta Potential and X-ray photoelectron spectroscopic (XPS).

1.2 Objective

Goal of this research mainly focused on these 2 aspects:

1. To synthesize spherical, narrow size distribution and monodispersed Ni nanoparticles that can easily be tailored in the mean of size with facile, efficient and less expensive procedure.

2. To synthesize Ni@Au bimetallic structure by coating of as-synthesized Ni nanoparticles with Au element that can be applied in biomedical areas.

1.3 Scope of work

Synthesis of Ni nanoparticles have been carried out in EG with hydrazine as the reducing agent and NaOH as the pH controller. The parameters that have been selected to be studied for both synthesis in 60˚C and boiling point of EG were as follows:

- Effect of N_2H_4/ Ni^{2+} molar ratio

  - Molar ratio of N_2H_4/ Ni^{2+} starts from 5 to 30.

- Effect of addition sequence of reactants

  -Three methods of adding sequence include; mix all reactants in room temperature and two hot temperature methods

- Effect of Ni^{2+}/OH^- molar ratio

  - Molar ratio of Ni^{2+}/OH^- include; synthesis without OH^- to molar ratio of 20

- Effect of reaction time

  - Reaction times were varied from 5 min to 2 hours

Selected Ni nanoparticles were then coated with Au for the synthesis of bimetallic particles. Magnetic behaviors of as-synthesized products were investigated as well to identify:

- Effect of size.

  - Magnetic analysis on particles sizes ranged 1 nm – 175 nm.

- Effect of different morphology.

  - Different morphology of chain-like and ball-like particles

- Au coated Ni nanoparticles.

  - Different between Ni nanoparticles without coating and with coating of Au.

CHAPTER 2

LITERATURE REVIEW

2.1 Introduction to nanotechnology

Richard Feynman's lecture on "There's plenty of room at the bottom" in 1959 herald a new idea of exploring the technology in nanoscopic size regime (Feynman, 1960). Shortly after that, many intensive works have been carried out for a better understanding on this small science, big deal's idea. This has proven that the history of 'nanoscopic technology' had started for quite a long time ago, nevertheless it was only at 1974, the term ''nanotechnology'' appeared. It was coined by a professor of Tokyo Science University name Norio Taniguchi (Horenstein, 2009). According to ISO/DTS 80004-1, nanotechnology can be defined as application of scientific knowledge to control and utilize matter in the nanoscale, where properties and phenomena related to size or structure can emerge. It definition also can be expanded through certain research areas.

21st century witnesses the burgeoning era of nanotechnology and is believe to be the most promising technology in the next few years. This new technology has created industrial revolution in many countries for it potential exciting breakthrough and sustainable future. Malaysia for instant has recognized nanotechnology as the new emerging field since 2001, with a huge allocation of budget to encourage innovative research and creation among local companies and universities (Hasyim et al., 2009).

2.2 Nanoscale materials

Nanomaterial is defined as material with any external dimension or having internal or surface structure in the range from approximately 1 nm to 100 nm. (ISO/DTS 80004-1). 1 nm equals to 10^{-9} or 1 billionth of meter and that is equal to about width of five atoms (Poole and Owens, 2003).Whether we realise or not, the natural nanomaterials have always been around us from ever since, however the nanomaterials with respect to nanotechnology is the new materials created by man. Nanomaterials are most frequently compared with the width of human hair which is approximately 10^5 nm.

Due to their small dimensions, nanomaterials have extremely large surface area to volume ratio, which makes a large fraction of atoms of the materials to be the surface or interfacial atoms, resulting in more surface dependent material properties. Their chemical and physical properties dramatically depend on their size and shape. For instant, nanometer magnetic materials can exhibit superparamagnetic behaviour which provides great potential in many biomedical applications (Chen et al., 2007). Nanoscale materials also have been reported to have great potential in important other fields such as environmental application, cosmetic, consumers goods and so on.(Nagarajan, 2008, Kokura et al., 2010; Ilisz et al., 2004; Gao et al., 2009).

2.3 Ni: Bulk vs. nano

2.3.1 Overview

Pure bulk Ni is a lustrous white, hard and one of the four ferromagnetic elements at room temperature in transition metal group VIII of the Periodic Table. It has high ductility, good thermal conductivity, high strength and fair electrical

conductivity. Due to its unique mentioned properties, bulk Ni had been used as electroplating and metal alloys because of its resistance to corrosion and also in nickel-cadmium batteries; as a catalyst and for coins as well. Ni nanopaticles also are relatively stable in air compared to Co and Fe nanoparticles (Zhang et al., 2009).

2.3.2 Crystallite structure

It is well known, that Ni can exist in two crystallite structure, name as face centered cubic (FCC), and hexagonal close packed (HCP). FCC Ni is stable in low temperatures below 300˚C, where else HCP is a structure that stable in high temperature. However HCP structure is rarely found due to the difficulties in synthesizing it. Ni nanocrystals have a strong tendency to form particles with FCC structure as it is the most stable structure for Ni compare to HCP (Hou et al., 2005). FCC Ni is ferromagnetic in room temperature. The typical electron diffraction pattern of Ni nanoparticles is shown in Figure 2.1. The five fringe patterns are related to the (111), (200), (220), (311) and (222) planes of pure FCC Ni. However in most works, FCC Ni is recorded in the range of (111), (200) and (220).

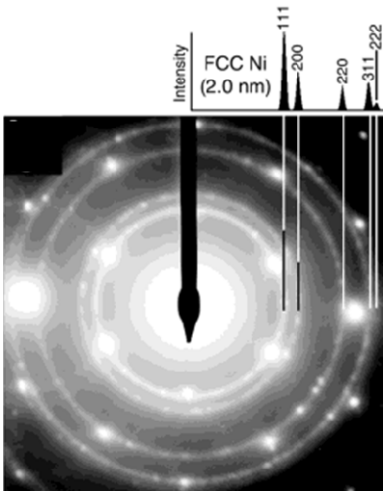

Figure 2.1 Selected-area electron diffraction (SAED) pattern of FCC Ni nanocrystallites with size of 2 nm (Zach and Penner, 2000).

One of the easiest and fastest ways to identify Ni nanomaterials formation is through X-ray diffraction pattern. Figure 2.2 represent the XRD patterns that have been reported by Abdel-Aal et al. (2007) in preparing Ni nanopowders via hydrothermal reduction method. Figure 2.2 (b) shows the formation of three peaks at 2θ at 44.5, 51.8 and 76.4 (JCPDS-04-0805) which corresponding to the (111), (200) and (222) lattice planes revealing that as-synthesized product is pure Ni element with a FCC structure. There are also possibilities that as-synthesized product is a mixture of Ni and by-product or impurity as been reported in Figure 2.2 (a) that shows the presence of hexagonal $Ni(OH)_2$.

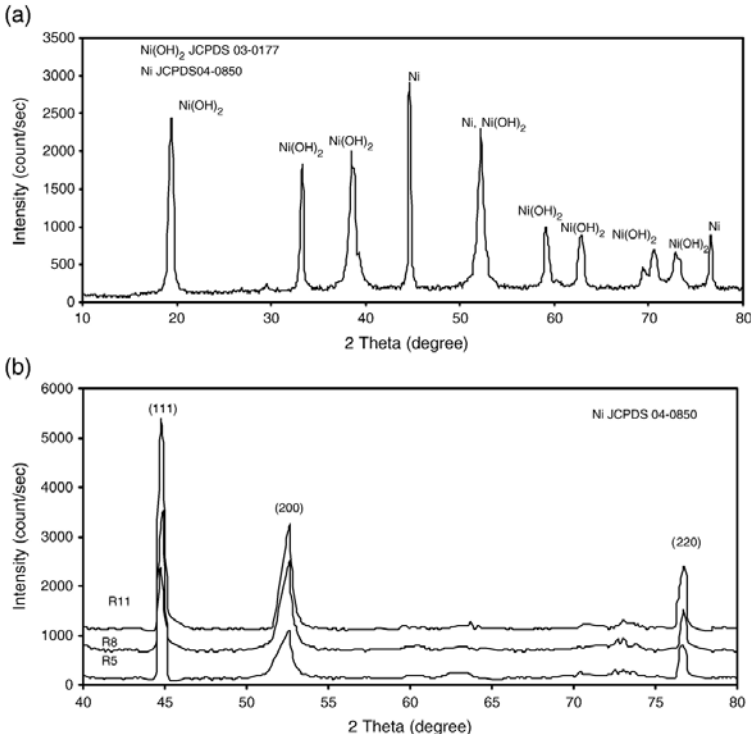

Figure 2.2 XRD patterns of (a) Ni and $Ni(OH)_2$ mixture and (b) pure Ni (Abdel-Aal et al., 2007).

XRD pattern can also provide us with information to obtain the crystallite size of as-synthesized particles. Crystallite sizes of samples were estimated from full-width at half-maximum (FWHM) of Ni (111) peak using the well-known Scherrer equation as in Equation 2.1.

$$L = \frac{K\lambda}{\beta \cos\theta} \tag{2.1}$$

where L is the average crystallite size, K is the Scherrer constant related to the shape calculated as 1 for spherical size, index (h k l) of the crystals, λ is the wavelength (0.154056 nm) of the x-rays, is the additional broadening (in radians) and θ is the Bragg angle. Line broadening of XRD peaks was used to estimate the average crystallite size.

Nevertheless, there are many conflicts on the values obtained with this calculation. As it is well known, in most condition crystallite size will not be the particle size, as particles may also exist as a group of crystallite, so the values obtained from FWHM are usually smaller than the TEM results (Wang et al., 2008). There are also cases where calculated crystallite size from FWHM of the x-ray diffraction peaks bigger than the size from TEM observation, which may be due to small number of large crystallites mixed with a much larger number of crystallites. Three well known causes of line broadening are small crystallite size, nonuniform strain and stacking faults (Cullity and Stock, 2001; Zach and Penner, 2000). We may also need to consider the instrumental error and lattice distortion that may influence the final result. We may say that calculated crystallite size from FWHM only give us inaccurate values which can be used to see the different between each experiment

condition but not the actual values. Therefore in this work, crystallite size will not be considered to avoid any confusions of calculated crystallite size from FWHM and observed particles size from TEM, unless there are difficulties to obtain result from TEM.

2.3.3 Ni nanostructures particles

Synthesis of nanosized Ni with various shapes and morphologies has attracted much attention because of the potential improvement of their properties such as in chemical and electrical. In some cases new properties were realised. Several examples of Ni nanostructures particles are shown in Figure 2.3. These structures were prepared by a variety of methods including low temperature chemical reduction in aqueous solution (An et al., 2009), microemulsion using CTAB as surfactant (Hu and Sugawara, 2008), microemulsion in CTAB/octane (Zhang et al., 2005), solvothermal at 100˚C (Tian et al., 2008), in ethylene glycol with hydrazine as reducing agent (Wang et al., 2008; Yu et al., 2003). Several factors that could affect the final morphology of as synthesized products are method of preparation and environment in solution.

Another type of Ni nanostructures is nanostructures that consist of Ni nanoparticles usually spherical in shape that self-assemble to form new structures. This unique phenomenon of self—assemblies act differently depending on method of preparations. Under certain environment Ni nanoparticles tend to form secondary particles which are the results of van der Waals attractive forces (Chou and Huang, 2001) and magnetic dipole interactions as well as thermodynamic driving force (An et al., 2009). The high surface area and magnetic properties of nanosized Ni also

contribute to the self-assembly formation. Figure 2.4 represents self-assembly of Ni nanoparticles forming different shapes and morphologies that have been synthesized with variety of methods.

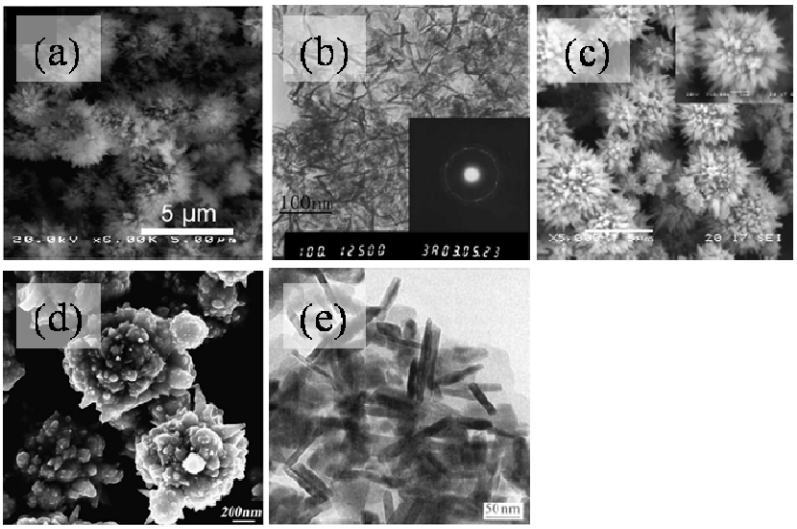

Figure 2.3 Ni nanostructured have been synthesized with the following shapes: (a) Sea urchin-like Ni, (b) Needle-like Ni, (c) Dandelion-like Ni, (d) Ni flowerlike, (e) Ni nanorod (Modified from Hu and Sugawara, 2008; Zhang et al., 2005; Tian et al., 2005; Wang et al., 2008; Yu et al., 2006)

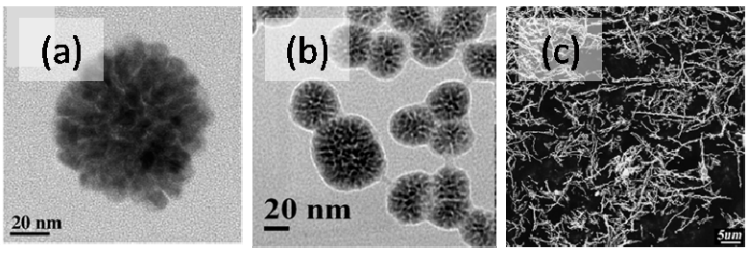

Figure 2.4 Ni self-assembly of (a) nanoflowers, (b) snow-ball flower, (c) nanowires (Modified from Xu et al., 2008; Mandal et al., 2009; Wang et al., 2009)

2.4 Synthesis of metal nanoparticles

2.4.1 Overview

Synthesis of nanoscale materials is the most important prerequisite in building of nanoblocks towards fabrication of functional devices in nanotechnology. Figure 2.5 illustrates two main approaches of nanoscale material, which can be identified as bottom-up and top-down approach. Top-down approach is breaking down a system into sub-system that usually involved mechanical size reduction such as grinding or milling. The advantage of the top down is it can produce large quantity of NPs but not uniformed in size.

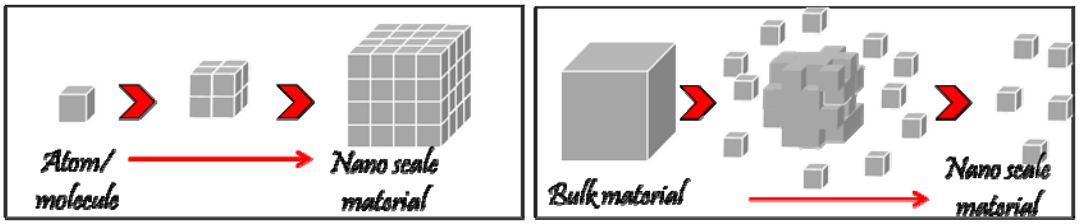

Figure 2.5 Model representation of (a) Bottom-up approach and (b) Top-down approach

On the other hand, bottom-up approached is a piecing together of system to a bigger system which usually involve chemical reaction such as wet chemical synthesis. Bottom-up approached have been extensively used as the synthetic method of producing nanomaterials with an advantage of more controllable of as-synthesized products. Utilizing bottom-up approached, the preparation of nanoparticles can be achieved through various methods. Synthesis of precious elemental nanoscale particles such as Co and Ni can be challenging attempts compare to metal oxide nanoscale materials synthesis because of several limitations such as their tendency to oxide spontaneously when exposed to air.

2.4.2 Preparation of Ni nanoparticles

Ni nanoparticles have been synthesized through various methods. To date several methods of synthesis that have been reported previously in the literature such as reverse microemulsion, microwave-assisted, solvothermal, water-in oil-emulsion, hydrothermal, laser-driven decomposition and polyol method (Chen and Wu, 2000; Zhang et al., 2005; Ai et al., 2003; Xu et al., 2008; Xu et al., 2007; Zhang et al., 2008; Li et al., 1999; Abdel-Aal et al., 2007; He et al, 2005; Wu and Chen, 2003). Of all methods, wet chemical synthesis through chemical reaction of metal salts is the most favourite method for the preparation of nanoscale materials for it facilely, economically, and flexibility to control the reaction environment as well as the final products (Hyeon, 2003).

2.4.3 Microemulsion method

Microemulsion are colloidal 'nano-dispersions' of either water-in-oil or oil-in-water) stabilized by interfacial film of surfactant molecules **(**Lopez-Quintela, 2003). The first work reported using reaction in microemulsions was by Boutonnet et al (Li and Park, 1999) Preparations of nanomaterials through microemulsion method usually involve chemical reduction or chemical deposition by mixing two microemulsions containing different solutes (Zhou et al., 2006). This technique has been used as chemical reactors because of their special interfacial properties of hydrophilic and hydrophobic domains at nanoscale level (Lopez-Quintela et al., 2004). Several works that reported the used of micoemulsion method to synthesis nanoparticles are in the synthesis of nanoparticles such as Ni (Chen and Wu, 2000), Cu (Qiu e al., 1999), as well as bimetallic structure (Chen et al., 2007),(Han et al., 2008).

2.4.4 Polyol Method

Polyol method has been developed in 1980's by Fievet et al in an attempt to synthesis fine metal powders (Grisaru et al., 2003). Polyol synthesis presents added advantages for the production of monodispersed metallic nanocrystals with a controlled particle size at nanometer scale, energy-efficient and environmentally friendly process as the reaction is carried out under closed system conditions compared to some syntheses methods that use noxious compound. It is also a cost-effective method, feasible and suitable for scaling up compare to any other methods which involve the use of expensive and noxious compound as well as complicated process (Kurihara et al., 1995). Besides that, it is also not as susceptible to impurities as another method.

Polyol method have been widely applied to synthesize metallic particles such as Ru, Rh, Sn, Re, W, Pt, Pd, Au, Fe, Ir, Ni, Co (Bonet et al., 1999; Chen et al., 2008; Patel et al., 2005; Lee et al., 2006; Hinotsu et el., 2004). It usually involves the use of poly-alcohol as both solvent and reducing agent (Coute et al., 2007). The poly-alcohol can be ethylene glycol (EG), diethylene glycol (DEG), tetramethylene glycol (TMEG), ethylenediamine tetraethylene glycol or 1, 2- propanediol (Hinotsu et al., 2004; Mi et al., 2005). Each of the poly-alcohol has their own reduction potential thus produced different yield and particles size (Joseyphus et al., 2007). Joseyphus et al. (2007) estimated the reduction potential of polyol by considering the relative levels of highest occupied molecular orbital (HOMO), lowest unoccupied molecular orbital (LUMO) and metal salts singly occupied molecular orbital (SOMO) of polyol and metal. It suggested that EG has lower value (-9.111 eV) compared to TMEG (-8.903 eV) as in Figure 2.6.

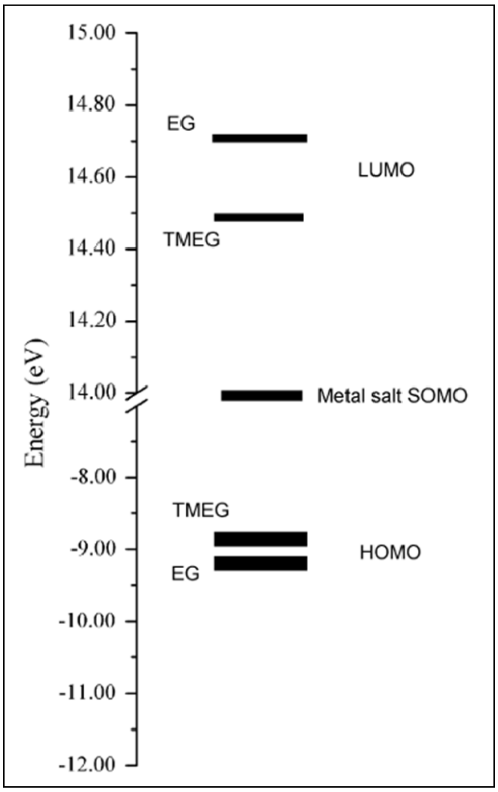

Figure 2.6 The HOMO and LUMO energy levels for TMEG and EG on comparison with SOMO for metal salts (Joseyphus et al., 2007).

Among all of the poly-alcohol, EG is the most commonly used due to its high electric constant and high reduction ability (Li et al., 2005). EG has less number of carbon atoms in a molecule among other glycols in the polyol, it can easily be removed by washing with ethanol or acetone. It is believed, that the dissolution of metal salt in EG at room temperature yield colloidal metal dispersion but kinetic is very slow (Lee et al., 2006). Li et al (2005) found that at high temperature, EG will decomposed to generate some kind of reducing agent for reduction of metallic ions to metal. Mechanism of reduction of metal ions by EG may probably involved the following reactions:

$$HOCH_2CH_2OH \rightarrow CH_3CHO + H_2O \quad (2.1)$$

$$nCH_3CHO + M^{n+} + H_2O \rightarrow n/2CH_3COCOCH_3 + M^0 + nH^+ \quad (2.2)$$

(M = Co, Ni).

This mechanisms of reduction have been repeatedly stated in numbers of research work where the first step (Equation (2.1)) is the degradation of EG to acetaldehyde followed by duplicative oxidation at step 2 (Equation (2.2)) (Joseyphus et al., 2007, Kim et al., 2009). Decomposition of EG to acetaldehyde are then acts as a reducing agent in the synthesis of metal particles. It had also been suggested by Hedge et al (1997) that EG may adsorbed to the surface of particles to prevent undesired surface oxidation. Kim et al (2009) proposed that reaction process in polyol should go through different stages of formation of $Metal(OH)_2$, dissolution of it in polyol, followed by reduction, nucleation and finally growth that will either through agglomeration of smaller particles or growth to a bigger but dispersed particles, depending on the environment in reaction (Figure 2.7). Hinotsu et al (2004) on the other hand reported that TMEG enhanced the reaction kinetic in the synthesis of Ni nanoparticles.

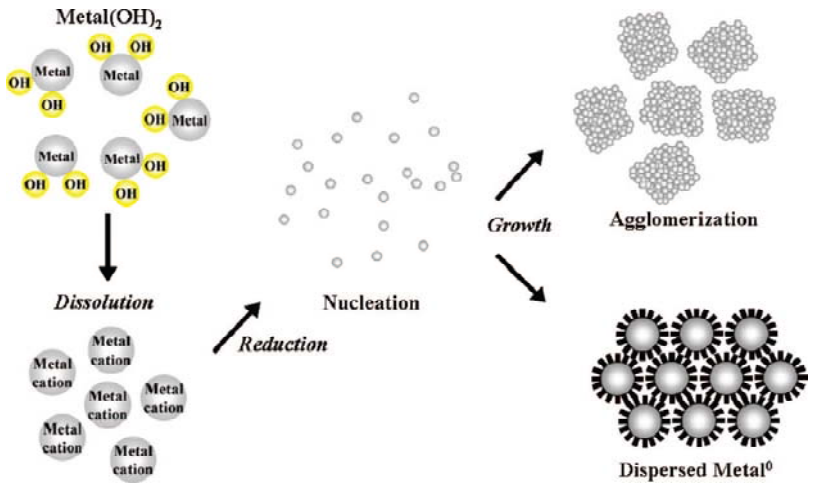

Figure 2.7 Schematic presentation of the different stages of the reaction process in polyol synthesis. (Kim et al., 2009)

According to Kodoma et al. (2007) reaction rate, r can be defined by

$$r = f(P_{redox}, C_{metal}, C_{OH}, T) \quad (2.2)$$

where P_{redox} is reduction potential of polyol, C_{metal} is concentration of precursor, C_{OH} is concentration of hydroxyl ions and T is temperature of reaction. When the P_{redox} of the polyol system is high, more nuclei will form and the particles size is consequently small due to limited supply for further growth. The reaction rate can also be enhanced with the increased of C_{metal}. In addition, the concentration of hydroxyl ions plays a big role as a catalyst in reduction process in polyol (Wu and Chen, 2003). Temperature as well influences the rate of reaction in polyol system.

2.5 Influence of experimental parameters on the synthesis of Ni and other magnetic nanoparticles

2.5.1 Overview

Optimization of synthesis parameter is always been an interesting research area in the attempt to create better production strategy of nanomaterials. Synthesis of precious metal such as Co and Ni can be very challenging compared to metal oxide nanoscale particles synthesis because of cumbersome limitations such as oxidation and their tendency to agglomerate. By appropriate tuning of several synthesis parameters including reaction temperature, time, concentration, pH and capping agents, in turn allow tailoring of nanoparticles in a broad range. This include of not only size but also the morphologies and structures. Studies to date have shown that with a good control of the synthesis, it may be possible to synthesis products according to our need.

2.5.2 Effect of Temperature

Synthesis of nanomaterials particularly Ni nanoparticles, have been carried out in wide range of temperature in which, most of them need heating of solutions. It has been proven from related reports on the synthesis of various metal nanoparticles, that every element may have different reaction temperature depends on the methods of synthesis and also their reducing potential.

Conventional polyol method uses relatively high boiling point polyol between 120-200˚C to synthesis fine metallic powder (Hegde et al., 1996; Kurihara et al., 1995). As discussed before decomposition of EG at high temperature would enhance the reduction process add (Li et al., 2005). Synthesis of nanoparticles as low as room temperature (25˚C), have been reported but they were either required the used of very strong reducing agents or an additional heat treatment to improve the crystallinity (Alonso et al., 2005; Wu et al., 2009; Duan and Li, 2004; Zheng et al., 2001).

For Ni nanoparticles synthesis, interestingly, there are number of work been reported on the synthesis of Ni nanoparticles in polyol or aqueous with reducing agent carried out at temperature of 60˚C and above. (Liu et al., 2008; Bai et al., 2008; Park et al., 2006; Kim et al., 2004; Wu and Chen, 2003; Yu et al., 2003). These findings suggest that 60˚C is a unique starting temperature for the synthesis of Ni nanoparticles. Wu and Chen (2003) for instant reported that if reaction temperature is lower than 60˚C, no reaction will took place.

Temperature of reaction also gives big influences on the particles size. Based on report of Shevchenko et al (2003) on the effect of temperature on particles size, synthesis of nanoparticles proceeds in few stages as shown in Figure 2.8. According to Shevchenko et al higher rate of nucleation will lead to smaller size of particles, which depend strongly to temperature of reaction rather than the growth rate. Bai et al (2008) also reported that higher temperature leads to smaller particles size as more nuclei formed at the initial stage of the reaction that restrained the growth of particles. Wang et al (2008) on the other hand, explained formation of larger particles at low temperature is because the reaction was slow thus very little nucleus were produced and finally aggregated together in the growth process. Nevertheless, there were also reports on an increased of particles size with increasing of temperature (Hu and Sugawara, 2009; Kim et al., 2004; Hyeon, 2002; Kurihara et al., 1995).

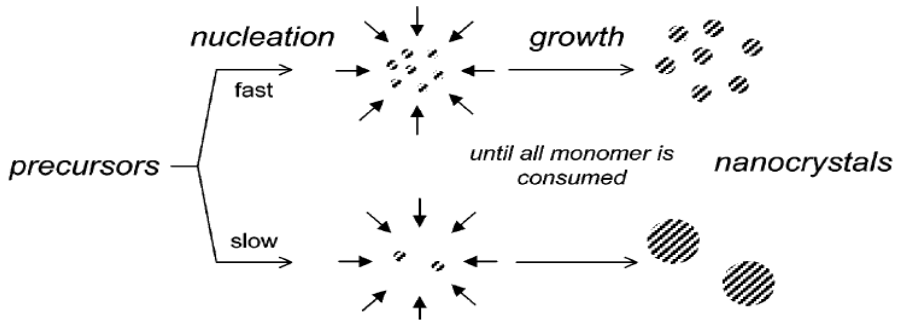

Figure 2.8 Schematic representation of nanoparticles synthesis (Shevchenko et al., 2003)

In recent years, synthesis of Ni nanostructures in various morphologies as in Figure 2.3 have been reported. It is believed, temperature play a big roles in the formation of this new morphologies. Tian et al (2008) synthesized dandelion-like Ni nanostructures in polyol at temperature of 100˚C. Ma et al (2008) have likewise reported the production of sea-urchin-like Ni nanostructures at 80˚C in aqueous,

however when the temperature was changed to 60-70˚C, chain-like Ni nanostructures were formed.

2.5.3 Effect of pH

The pH of the solution is frequently been address as one of the important parameter in preparation of nanoparticles. Several chemicals have been used as pH adjuster such as sodium bicarbonate ($NaHCO_3$) and sodium carbonate (Na_2CO_3) (Lee et al., 2006; Li e al., 1999). The most common pH adjuster is sodium hydroxide (NaOH) that have been reported to act as a catalyst to enhance the reduction rate in the synthesis of various metals such as Ni and Co, thus reduced the size of as-synthesized nanoparticles (Wu and Chen, 2003; Wang et al., 2008; Kurihara et al.,1995). In polyol, OH^- ions enhance the decomposition of EG to acetaldehyde (Sun et al., 2005). Moreover, high viscosity mixture of NaOH and ethylene glycol (EG) favour the high yield of as-synthesized particles and consequently prohibit aggregation of Ni nanoparticles for better dispersion (Wang et al., 2008).

NaOH addition was also found to influence the morphology of as-synthesized products significantly. An et al. (2009) synthesized various interesting Ni nanostructures with different concentration of NaOH in aqueous solution at 70˚C. This is believed to be the results of changing of reducing rate, velocity of nucleation and crystal growth as the concentration of NaOH been tailored. NaOH not only enhanced the reaction rate as been mentioned before, it also was found to control the aggregation and growth of the Ni crystallite (An et al., 2009). We can postulate that NaOH play a big role in the synthesis of metal nanoparticles.

2.5.4 Effect of reducing agent

There are a number of reducing agents that have been used to synthesis nanoparticles for instant hydrazine (N_2H_4), sodium borohydrite ($NaBH_4$) and sodium citrate ($Na_3C_6H_5O_7$). Besides that, there are also reports on synthesis of nanoparticle without using any reducing agents especially when using high boiling temperature polyol (Hinotsu et al., 2004; Kurihara et al., 1995; Ying et al., 2005; Chou and Huang, 2001). However particles produced were in submicron size.

Hydrazine is the most commonly used reducing agents to reduce metal nanoparticles such as Ni and Co (Li et el., 1999; Yu et al., 2003; Wu and Chen, 2003; Kim et al., 2004; Kudlash et al., 2008; Zheng et al., 2000; Abdel-Aal et al, 2006; Sidhaye et al., 2009). It is cheap and usually produced product without contamination from reducing agent itself. A temperature dependent with chemically active free ion of hydrazium cation, ($N_2H_5^+$) is a strong reducing agent under basic medium and the reducing ability decreases with the decrease of pH(Park et al., 2006; Yu et al., 2003). Park et al express the reduction of Ni^{2+} with N_2H_4 in the present of NaOH composed of 3 reactions:

$$Ni^{2+} + N_2H_4 + 4OH^- \rightarrow 2Ni\downarrow + N_2\uparrow + 4H_2O \quad (2.3)$$

$$N_2H_4 \rightarrow N_2\uparrow + 2H_2\uparrow \quad (2.4)$$

$$3N_2H_4 \rightarrow N_2\uparrow + 4NH_3 \quad (2.5)$$

According to stoichiometric in equation (2.3), reaction will proceed when molar ratio N_2H_4/Ni^{2+} =0.5. However because of side reaction of N_2H_4 decomposition catalyzed by Ni surface, into N_2, H_2 and NH_3 on heating as in equation (2.4) and (2.5), no

reaction will take place when molar ratio N_2H_4/Ni^{2+} =0.5 is used. Therefore to ensure reduction take place, molar ratio have to be higher than 0.5.

Commonly when the molar ratio increase, reaction rate also increase. Wu and Chen (2003) reported how the particles size decrease with increasing of N_2H_5OH /Ni^{2+} molar ratio, but remained unchanged when > 12. This finding suggested that when the molar ratio reached certain value where nucleation rate can no longer be improved, the particles size will be constant at the smallest value. On the contrary, Park et al reported that when N_2H_4 concentration was too high, non-spherical and highly agglomerated particles with broad size distribution was produced.

2.5.5 Effect of reaction time

Reaction time is also one of the major factor that influences the final product in the synthesis of nanoparticles. In order to achieve high yield and pure nanomaterials, sufficient reaction time is necessary (Bai et al., 2008). Park et al., reported that before reaction time of 6 minutes, $Ni(OH)_2$ and mixture of $Ni(OH)_2$ and Ni metal was detected which suggest that synthesis of Ni nanoparticles involved the formation of $Ni(OH)_2$ from nickel hydrazine complex as the intermediate product.

Prolonged of reaction time is believe will increased the particles size via particles growth and Ostwald ripening. Ostwald ripening is a process where small particles dissolved followed with the growth of large particles thus increase in particles size (Wang et al., 2008) (Figure 2.9).

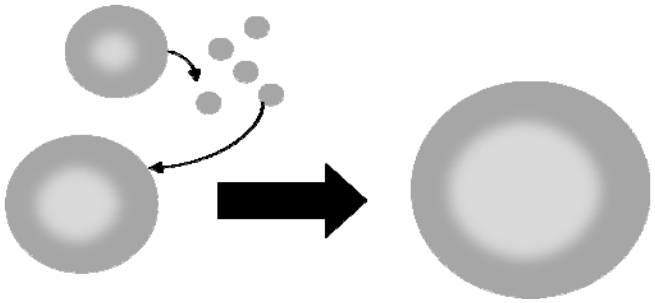

Figure 2.9 Schematic of Oswalt ripening process.

2.5.6 Effect of metal precursor concentration

The metal precursor concentration can give big influences on particles size and their morphologies. According to equation (2.4), reduction rate will increase with the increase of metal precursor concentration. Theoretically we would expect smaller size of particles size as reduction rate increase, nevertheless based on the works reported previously this did not happened.

According to Wang et al (2008), at very high concentration of Ni^{2+}, reaction was very fast which resulted weakened of the crystallinity thus resulted the change of morphology from spherical to flowerlike that consist of smaller spherical particles. The particles size also increased with increased of Ni^{2+} concentration that contradicted theory which stated that higher reaction rate produce smaller particles size. Wang et al explained that at the beginning of reaction very few nuclei were formed and firstly precipitate which acted as self catalytic that enhanced the reaction. As a result the particles size increased because there were still many Ni atoms left in solution that involved in growth process. However when the concentration is too low, no particles could be obtained as there were not enough atoms to form stable nucleus, while when it is too high and would end up producing bigger particles or forming $Ni(OH)_2$ and Ni mixture. On the other hand, Wu et al (2009) explained the increased